OXFORD

ORIGINAL ARTICLE

Prevention of prostate cancer by natural product MDM2 inhibitor GS25: *in vitro* and *in vivo* activities and molecular mechanisms

Wei Wang[1,2,3,*], Jiang-Jiang Qin[1,3], Xin Li[1,3], Guanyu Tao[1,3], Qiang Wang[3,4], Xuming Wu[5], Jianwei Zhou[4], Xiaolin Zi[6,7] and Ruiwen Zhang[1,2,3]

[1]Department of Pharmacological and Pharmaceutical Sciences, College of Pharmacy, University of Houston, Houston, TX 77204, USA, [2]Center for Drug Discovery, University of Houston, Houston, TX 77204, USA, [3]Department of Pharmaceutical Sciences, School of Pharmacy, Texas Tech University Health Sciences Center, Amarillo, TX 79106, USA, [4]Department of Molecular Cell Biology and Toxicology, School of Public Health, Nanjing Medical University, Nanjing 210029, China, [5]Nantong Center for Disease Control and Prevention, Nantong 226000, P.R. China, [6]Department of Urology, University of California, Irvine, CA 92868, USA and [7]Department of Pharmacology, University of California, Irvine, CA 92868, USA

*To whom correspondence should be addressed. Tel: +1 713 743 7349; Fax: +1 713 743 1229; Email: wwang4@central.uh.edu
Correspondence may also be addressed to Ruiwen Zhang. Tel: +1 713 743 6840; Fax: +1 713 743 1229; Email: rzhang27@central.uh.edu

Abstract

Prostate cancer remains a major health problem in the USA and worldwide. There is an urgent need to develop novel approaches to preventing primary and metastatic prostate cancer. We have identified 25-OCH$_3$-protopanaxadiol (GS25), the most active ginsenoside that has been identified so far; it has potent activity against human cancers, including prostate cancer. However, it has not been proven if GS25 could be a safe and effective agent for cancer prevention. In this study, we used the TRAMP model and clearly demonstrated that GS25 inhibited prostate tumorigenesis and metastasis with minimal host toxicity. Mechanistically, GS25 directly bound to the RING domain of MDM2, disrupted MDM2–MDMX binding and induced MDM2 protein degradation, resulting in strong inhibition of prostate cancer cell growth and metastasis, independent of p53 and androgen receptor status. In conclusion, our *in vitro* and *in vivo* data support the potential use of GS25 in prevention of primary and metastatic prostate cancer.

Introduction

Prostate cancer poses a major public health problem in the USA and worldwide. Although the current therapeutic modalities, such as radical prostatectomy, local radiotherapy and brachytherapy, can successfully control localized prostate cancer, they are often ineffective against metastatic and/or hormone-refractory prostate cancers (1–3). Unfortunately, there are limited effective approaches to prevent prostate cancer, and patients often remain asymptomatic until the disease is advanced and/or metastatic. Chemoprevention has been increasingly emphasized as an approach to mitigate the prostate cancer burden. Although many chemopreventive strategies (e.g. those involving selenium, vitamin E and inflammation blockade) have been

explored (4,5). 5α-reductase inhibitors (5-ARIs) have been shown to decrease the risk of prostate cancer (6,7) but are accompanied by an increased risk of high-grade tumors in large Phase III, randomized, placebo-controlled clinical trials (8,9). These 5-ARIs do not have a favorable risk-benefit profile for prostate cancer chemoprevention (8). Other interventions on the horizon, including dietary nutrients and pharmacological treatments, may hold some promise, but it is currently unclear whether any of these will be able to transition to clinical use. Therefore, there is an urgent unmet medical need to develop novel agents that can prevent the onset, development and progression of prostate cancer.

Abbreviations

GS25	25-OCH$_3$-protopanaxadiol
5-ARIs	5α-reductase inhibitors
MEF	mouse embryonic fibroblast

There is extensive evidence supporting the roles of oncogenes in carcinogenesis and cancer development and progression. As a major oncogene, MDM2 is amplified and/or overexpressed in prostate cancer, and has been linked to a poor prognosis and metastasis among patients with prostate cancer ([10,11]). MDM2 is a major negative regulator of p53 ([12]); it directly binds to p53, represses its transactivation activity ([13,14]), and promotes its degradation ([15,16]). However, we and others have demonstrated that MDM2 also has numerous p53-independent functions ([17–19]). In *in vitro* and *in vivo* models of prostate cancer and human prostate cancer patients, MDM2 has been demonstrated to promote cell growth, metastasis and tumor angiogenesis, regardless of the status of the androgen receptor and p53 in the cancer cells ([20–25]). These findings indicate that MDM2 is a valid target for prostate cancer prevention and treatment ([26]). Several pharmacological strategies targeting MDM2 have been tested, with the majority of the small molecule MDM2 inhibitors designed to inhibit the binding of MDM2 and p53 ([27,28]). Since these MDM2 inhibitors require the presence of wild-type p53 in order to affect the target cells, these agents would be expected to have little or no activity against cancers with a p53 deficiency (estimated to be 50% of all cancers) ([26,27]). Therefore, novel approaches to target MDM2 in a p53-independent manner represent a new direction for the design and development of MDM2 inhibitors for cancer prevention and therapy.

In recent years, dietary botanicals have become an important source of effective compounds for the treatment of cancer ([29,30]). Among them, extracts of ginseng have long been used as an herbal medicine and dietary supplement, and have been documented to provide various health benefits ([31]). They have also been reported to have prophylactic and therapeutic effects against several cancers ([31]). Numerous studies have indicated that the ginsenoside class of compounds is responsible for most of the anticancer activities of ginseng ([31]). We have discovered a ginsenoside, 25-OCH$_3$-protopanaxadiol (GS25), which shows significant *in vitro* and *in vivo* anticancer activities in prostate cancer models, with minimal host toxicity ([32,33]). In fact, this compound is the most active ginsenoside that has been identified so far ([32]). GS25 inhibits cell proliferation, induces cell cycle arrest and apoptosis, inhibits cell migration, inhibits tumor growth and metastasis *in vivo* and sensitizes prostate cancer cells to chemotherapy and radiation therapy, without causing any host toxicity ([33]). Interestingly, MDM2 downregulation is, at least in part, responsible for the observed cytotoxic effects of GS25 ([33]). In this study, we demonstrate the safety and efficacy of GS25 for preventing primary prostate cancers, and describe the primary molecular mechanisms of action. These data provide a strong basis for further investigating this newly discovered compound as a potential prostate cancer preventive agent with a novel mechanism of action.

Materials and methods

Chemicals, plasmids, siRNA and other reagents

GS25 ([32]) and biotinylated GS25 (biotin-GS25) were purified and synthesized by our laboratories, and the structures were confirmed by UV, IR, MS and NMR spectroscopy. All chemicals and solvents used were of the highest analytical grade available. Antibodies, plasmids and siRNAs were obtained commercially or were provided by other investigators; a detailed list is provided in the Supplementary Methods, available at *Carcinogenesis* Online.

Cell lines

Human prostate cancer LNCaP, PC3 and DU145 cell lines were obtained from the American Type Culture Collection (ATCC) and were cultured as described previously ([32,33]). Normal human prostate RWPE-1 cells were kindly provided by Dr. B. Guo (University of Houston, Houston, TX). The MDM2$^{-/-}$ p53$^{-/-}$ and MDMX$^{-/-}$ p53$^{-/-}$ mouse embryonic fibroblast (MEF) cell lines were kindly provided by Dr. G. Lozano (University of Texas, MD Anderson Cancer Center, Houston, TX) and were cultured in Dulbecco's modified Eagle's medium (DMEM). All cell culture media were supplemented with 10% fetal bovine serum and 1% penicillin/streptomycin. Frozen aliquots were used in experiments within 6 months of culture period, after the first thawing of the cells. Cell lines included in the study were validated by analysis of STRs (GenePrint® 10 System, Promega) and checked for mycoplasma contamination by polymerase chain reaction ([34]).

Assays for cell viability, colony formation, cell migration and cell invasion

The *in vitro* studies to evaluate the effects of GS25 on cell viability, colony formation, cell migration and cell invasion were performed using MTT, colony formation, wound healing and transwell invasion assays as described previously ([35,36]).

Molecular modeling

A molecular modeling study to predict the sites of GS25-MDM2 binding was performed using the SYBYL-X 2.0 software package (Tripos) ([35]). All of the docking results were analyzed using the Pymol 1.7 software as described previously ([35]).

Western blotting, immunoprecipitation and streptavidin–agarose pulldown assay

Cell lysates were collected in NP-40 buffer with a protease inhibitor mixture (Sigma). After centrifugation, the supernatants were collected and subjected to Western blotting as described previously ([35,36]). An immunoprecipitation assay was performed to examine the effects of GS25 on the MDM2–MDMX interaction as described previously ([35]). For streptavidin–agarose pulldown assay, the biotin-GS25-bound beads were incubated with the recombinant proteins and the bound proteins were detected as described previously ([35]).

Animal models and treatments

The animal protocol was approved by the Institutional Animal Use and Care Committee (IACUC). The animal experiments were strictly carried out according to the guidelines of the IACUC. Male transgenic C57BL/6-Tg (TRAMP) 8247Ng/J×FVB/NJ) F1/J mice and their male wild-type (WT) littermates were purchased from The Jackson Laboratory (Bar Harbor, ME). Briefly, 5-week-old male TRAMP mice were randomized into the following groups: TRAMP-control (vehicle only; *n* = 31), TRAMP-10 mg/kg GS25 (*n* = 28) and TRAMP-20 mg/kg GS25 (*n* = 28). The 5-week-old male WT littermates were given either the vehicle control (*n* = 6) or GS25 (20 mg/kg) (*n* = 6). GS25 was administered by i.p. injection at doses of 10 and 20 mg/kg/d (5 days/week) for 24 weeks. The mice were weighed weekly. After 24 weeks of treatment, plasma, various tissues (urogenital tract, prostate, liver, heart, lungs, kidneys, spleen and brain) and tumors were collected at necropsy. Prostates were dissected into coagulating gland, seminal vesicle, lateral, dorsal and ventral prostate and fixed with 10% buffered formalin. Tissues were sectioned at 4–5 μm thickness for hematoxylin and eosin (H&E) staining ([35,36]) and immunohistochemical analysis ([35,36]).

Pathology evaluation

The immunohistochemical staining and H&E staining were performed ([35,36]). Briefly, tumors and various tissues were removed from mice, fixed in 10% formalin and embedded in paraffin. The tumor and tissue sections (5 μm thick) were then prepared, deparaffinized in xylenes, rehydrated and washed with PBS. The immunohistochemical staining of target proteins

was performed using biotinylated antibodies and then the sections were counterstained with hematoxylin, mounted and analyzed. For H&E staining, tissue sections were stained in Mayer's hematoxylin for 10 min and then stained with Eosin for 1 min. Finally, all of the sections were analyzed and imaged under a phase-contrast Olympus microscope (Olympus America Inc., Central Valley, PA).

Assays for toxicity-related plasma indicators

The whole blood was collected from the C57BL/6 mice treated with vehicle or GS25 by cardiac puncture and plasma was separated and used to analyze the plasma levels of aspartate amino transferase (AST), alanine amino transferase (ALT), total bilirubin (TBIL), blood urea nitrogen (BUN) and creatinine (CR).

Statistical analysis

For *in vitro* experiments, statistics were calculated using Prism software version 6 (Graph Pad Software Inc.). All quantitative data are presented as the means ± SEM from at least three independent experiments. The significance of differences between mean values was evaluated using Student's *t*-test. The statistical analyses of all *in vivo* data were performed with the SPSS 18.0 software program for Windows (IBM). Fisher's exact test was used to compare all groups for tumor incidence and one-way ANOVA followed by Dunnett's test was performed to compare control response (vehicle) with test response. A value of $P < 0.05$ was considered to be statistically significant.

Results

GS25 suppresses prostate cancer cell growth, migration and invasion independent of the p53 and AR status of the cells

GS25 exhibited potent cytotoxicity again the LNCaP (p53 wild-type, AR positive, PTEN *null*), PC3 (p53 *null*, AR negative, PTEN *null*) and DU145 (p53 mutant, AR negative, PTEN$^{+/-}$) prostate cancer cell lines, with IC$_{50}$ values of 9.6, 4.4 and 7.6 µM, respectively (Figure 1A). However, GS25 did not show apparent effects on the viability of normal prostate epithelial RWPE-1 cells, indicating that GS25 has a selective cytotoxicity for prostate cancer cells. This compound also inhibited the cell colony formation in a concentration-dependent manner in all three prostate cancer cell lines, regardless of their status of p53, AR or PTEN (Figure 1B). GS25 was further investigated for its effects on the cell migration and invasion. As shown in Figure 1C and D, GS25 markedly inhibited cell migration into wounded areas and decreased the number of invaded cells at lower concentrations (2.5 and 5 µM) in a p53-, AR- and PTEN-independent manner.

GS25 was then examined for its effects on the expression of MDM2 in prostate cancer cells. As shown in Figure 1E, GS25 significantly inhibited the protein expression of both MDM2 and MDMX, resulting in increased expression levels of wild-type p53 in LNCaP cells, PTEN in DU145 cells and p21 in all three cell lines. The compound also decreased the protein expression levels of AR and PSA in LNCaP cells in a concentration-dependent manner. No significant change was observed in the expression of mutant p53 in DU145 cells.

GS25 directly binds to MDM2 and promotes its ubiquitination

We next examined the ability of GS25 to bind the MDM2 protein. Based on the results from molecular docking studies, GS25 could bind the RING finger domain of MDM2 via interactions with ARG444 and LYS479 (Figure 2A and B). The 12-hydroxyl group of GS25 could directly interact with LYS479 via a hydrogen bond. In addition, GS25 might also form a hydrophobic interaction with ARG444 in MDM2. The binding of GS25 to the MDM2 protein was further

demonstrated using biotinylated GS25 (biotin-GS25, Figure 2C) and recombinant GST-MDM2 protein. As shown in Figure 2D, GS25 directly bound to the MDM2 protein but not the GST tag. The GS25-MDM2 binding was significantly inhibited by non-biotinylated GS25, further indicating a specificity of this binding. To determine whether GS25-MDM2 binding affects the MDM2 protein stability, we examined the effects of GS25 on the half-life of the MDM2 protein in LNCaP and PC3 cells. As shown in Figure 2E, GS25 treatment significantly shortened the half-life of MDM2 in both cell lines and prolonged the half-life of wild-type p53 in LNCaP cells. It was further observed that GS25 promoted MDM2 ubiquitination in both cell lines (Figure 2F). These results suggest that GS25 enhances MDM2 auto-ubiquitination. In support of this idea, GS25 markedly reduced the expression levels of wild-type MDM2. However, it did not affect the expression of the mutant MDM2 (C464A) lacking ubiquitin E3 ligase activity (Figure 2G).

### MDMX plays an important role in GS25-induced MDM2 degradation

It was hypothesized that the binding of GS25 to the MDM2 RING finger domain could inhibit the MDM2–MDMX interaction, leading to MDM2 auto-ubiquitination and degradation. We therefore examined the effects of GS25 on the MDM2–MDMX interaction. As shown in Figure 3A, a 2-h treatment with GS25 largely reduced the binding of MDM2 to MDMX. To further investigate the role of MDMX in GS25-induced MDM2 degradation, MDMX$^{-/-}$ p53$^{-/-}$ MEF cells were transfected with a Myc-MDMX plasmid and treated with GS25. As shown in Figure 3B, MDMX overexpression significantly increased the endogenous level of MDM2 and accelerated GS25-induced MDM2 degradation in MDMX$^{-/-}$ p53$^{-/-}$ MEF cells. However, the MDM2 overexpression did not lead to any obvious effect on GS25-induced MDMX degradation in MDM2$^{-/-}$ p53$^{-/-}$ MEF cells (Figure 3C). The importance of MDMX in GS25-induced MDM2 degradation was further confirmed in transient MDMX knockdown (KD) experiments. As shown in Figure 3D, MDMX KD largely reduced GS25-enhanced MDM2 ubiquitination and degradation in both LNCaP and PC3 cell lines, indicating that GS25 prompted MDM2 auto-ubiquitination and degradation by inhibiting the MDM2–MDMX interaction.

Knocking down both MDM2 and MDMX blocks GS25's anticancer activity

To assess the roles of MDM2 and MDMX in the antiprostate cancer activity of GS25, the LNCaP and PC3 cells were transfected with MDM2 siRNA, MDMX siRNA or both, followed by treatment with GS25. As shown in Figure 4A, silencing either MDM2 or MDMX markedly reduced the effects of GS25 on the expression of wild-type p53 and p21. However, neither MDM2 KD nor MDMX KD affected the inhibition of AR and PSA expression by GS25. Furthermore, silencing either MDM2 or MDMX also significantly reduced the inhibitory effects of GS25 on colony formation and cell invasion in both cell lines (Figure 4B and C). More importantly, silencing both MDM2 and MDMX almost completely blocked the GS25-induced expression of p53 and p21, as well as its antiprostate cancer activity (Figure 4B and C).

GS25 inhibits prostate tumorigenesis and metastasis in the TRAMP model

The cancer preventive efficacy of GS25 was evaluated in the TRAMP model. Euthanasia was necessary as early as 17 weeks due to the large size of tumors in the TRAMP mice. In the vehicle-treated group, 14 mice were sacrificed with palpable prostate tumors, which were found to weigh 4–9 g, before the planned
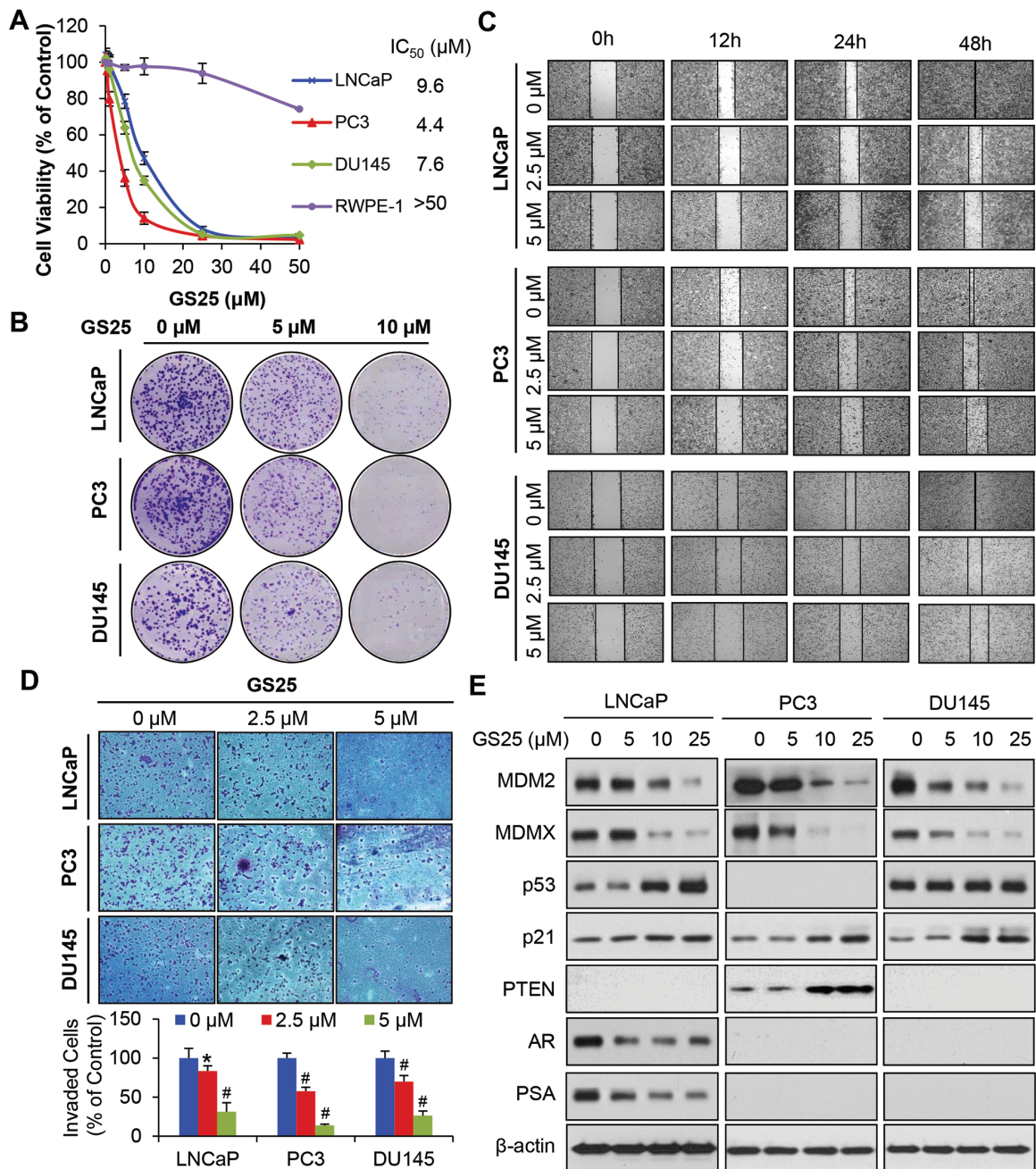
Figure 1. GS25 inhibits prostate cancer cell growth and metastasis by inhibiting MDM2, regardless of the p53 status and AR sensitivity. (**A–E**) LNCaP, PC3 and DU145 cells were treated with GS25 at the indicated concentrations for (**A**) 72 h for the MTT assay, (**B**) 24 h for the colony formation assay, (**C**) 48 h for the wound-healing assay, (**D**) 24 h for the transwell invasion assay and (**E**) 24 h prior to assessing the expression levels of various proteins by Western blotting. Data are representative of three or more experiments (*P < 0.05, #P < 0.01).

experiment terminal endpoint of 28 weeks of age. Only six and three mice in the GS25-10 mg/kg and GS25-20 mg/kg groups, respectively, were euthanized with tumors weighing 3–6 g, indicating that GS25 prolonged the survival of TRAMP mice (P < 0.01) (Figure 5A). In addition, GS25 also decreased the incidence of prostate cancer compared to the vehicle-treated group. As shown in Figure 5B, the incidences of palpable prostate tumors at 28 weeks of age were 20/31 (64.5%), 10/28 (32.3%) and 6/28 (19.4%) in vehicle, GS25-10 mg/kg and GS25-20 mg/kg groups, respectively. Approximately 48.4% (15 out of 31) mice in the control group showed lymph node metastases, whereas only 14.3% (4 out of 28) (P < 0.01) and 7.14% (2 out of 28) (P < 0.01) mice had

metastases in the GS25-10 mg/kg and GS25-20 mg/kg treatment groups, respectively. In addition, the treatment groups showed smaller metastatic lymph nodes (166.1 ± 39.4; 94.7 ± 33.9 and 12.3 ± 2.1 mg in the control, GS25-10 mg/kg and GS25-20 mg/kg groups, respectively). Interestingly, necropsy also showed that 5, 3 and 3 mice from control group developed metastatic lesions in the lungs, liver and kidney, respectively. However, no visible metastatic lesions were found in the GS25 treatment groups. These results were confirmed by histopathological evaluations.

We then evaluated the effects of GS25 on the total prostate weight. As shown in Figure 5C, prostate growth was inhibited by 44.9% (P < 0.01) and 55.0% (P < 0.01) at 28 weeks in the 10
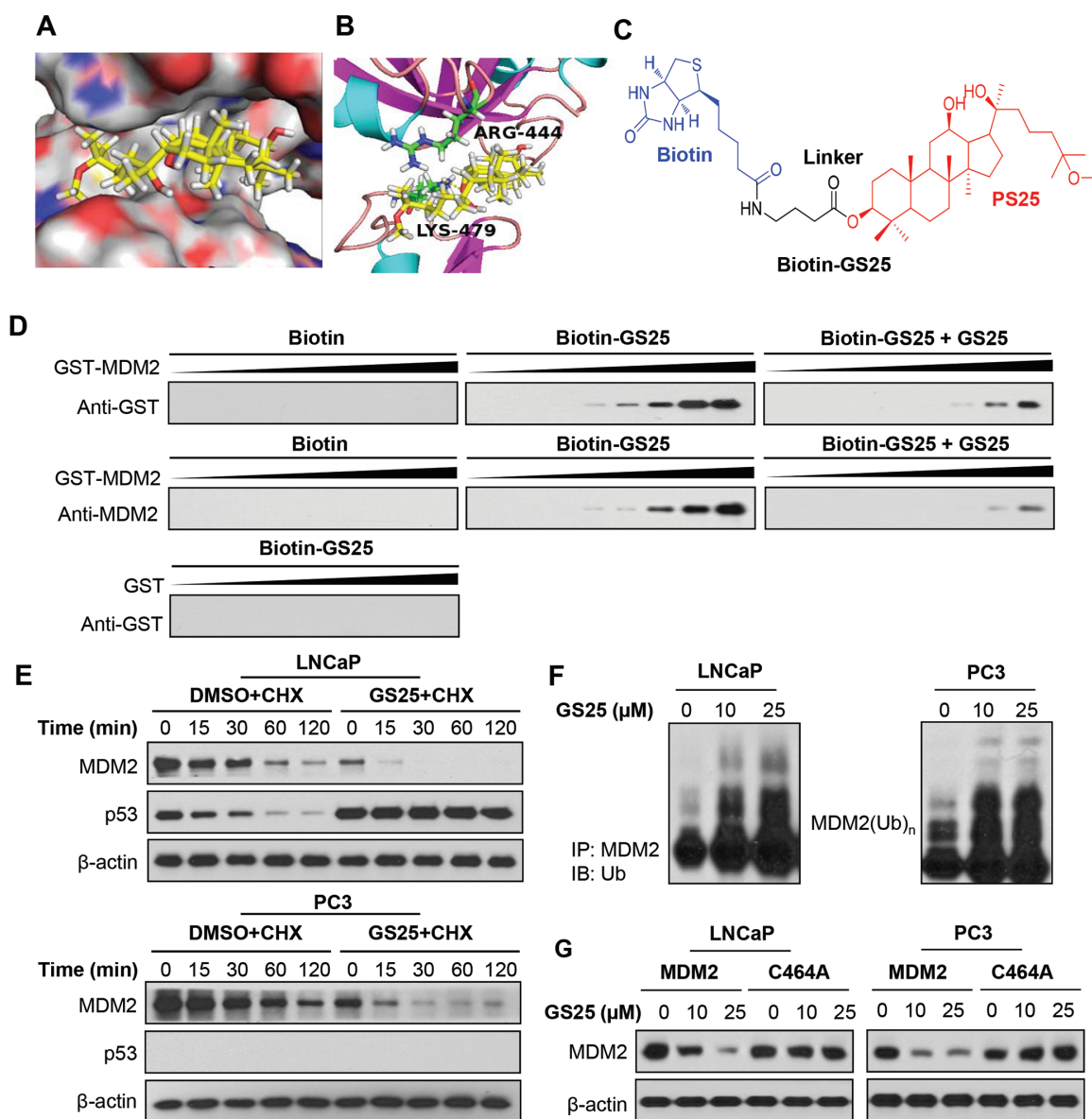
Figure 2. GS25 directly binds to and increases the auto-ubiquitination of the MDM2 protein. (**A**) Computational modeling of GS25 binding to the RING domain of MDM2. GS25 was rendered in yellow, with the atoms important for binding highlighted in red. (**B**) The predicted binding mode of GS25 with MDM2. The key residues interacting with GS25 were rendered as sticks. (**C**) The chemical structure of biotinylated GS25 (biotin-GS25). (**D**) Biotin-GS25-bound avidin beads were incubated with recombinant GST-MDM2 in the presence or absence of non-biotinylated GS25. The bound proteins were examined by Western blotting. GST was used as a negative control. (**E**) LNCaP and PC3 cells were treated with GS25 (10 µM) for 24 h, followed by exposure to a protein synthesis inhibitor, cycloheximide (CHX, 15 µg/ml). The protein expression levels of MDM2 and p53 were detected by a Western blot analysis at the indicated times after exposure to CHX. (**F**) LNCaP and PC3 cells were co-transfected with MDM2 and ubiquitin plasmids, followed by treatment with GS25 at the indicated concentrations for 24 h. Cell lysates were subjected to immunoprecipitation with an anti-MDM2 antibody. The ubiquitinated MDM2 was detected using an anti-ubiquitin antibody. (**G**) LNCaP and PC3 cells were transfected with a wild-type MDM2 plasmid or a mutant MDM2 plasmid (C464A) without E3 ligase activity, followed by exposure to GS25 at the indicated concentrations for 24 h, and the MDM2 levels were detected by Western blotting. Data are representative of three or more experiments.

and 20 mg/kg GS25 treatment groups, respectively. Similarly, 10 mg/kg of GS25 had moderate effects on the tumor burden, and a 24-week treatment led to ~47% inhibition of tumor growth (tumor weight) ($P < 0.01$). However, treatment for the same period of time using 20 mg/kg of GS25 inhibited tumor growth by 63% ($P < 0.01$) (Figure 5D).

GS25 decreases MDM2 expression and regulates metastasis-related protein expression in prostate and tumor tissues

We further examined the expression levels of MDM2 and MDMX and other metastasis-related proteins in both prostate and tumor tissues from the TRAMP model mice. Histopathological examinations of prostate tissue sections showed that GS25 treatment significantly reduced the expression levels of MDM2 and MDMX in a dose-dependent manner (Figure 5E and F). GS25 also increased the expression levels of p21 and E-cadherin, and decreased the expression level of β-catenin (Figure 5E and F). Consistent with the observations in prostate tissues, the inhibition of MDM2, MDMX and β-catenin, and the induction of p21 and E-cadherin, were also observed in prostate tumors (Supplementary Figure 1A and 1B, available at *Carcinogenesis* Online) and were confirmed by a Western blot analyses (Supplementary Figure 1C, available at *Carcinogenesis* Online).
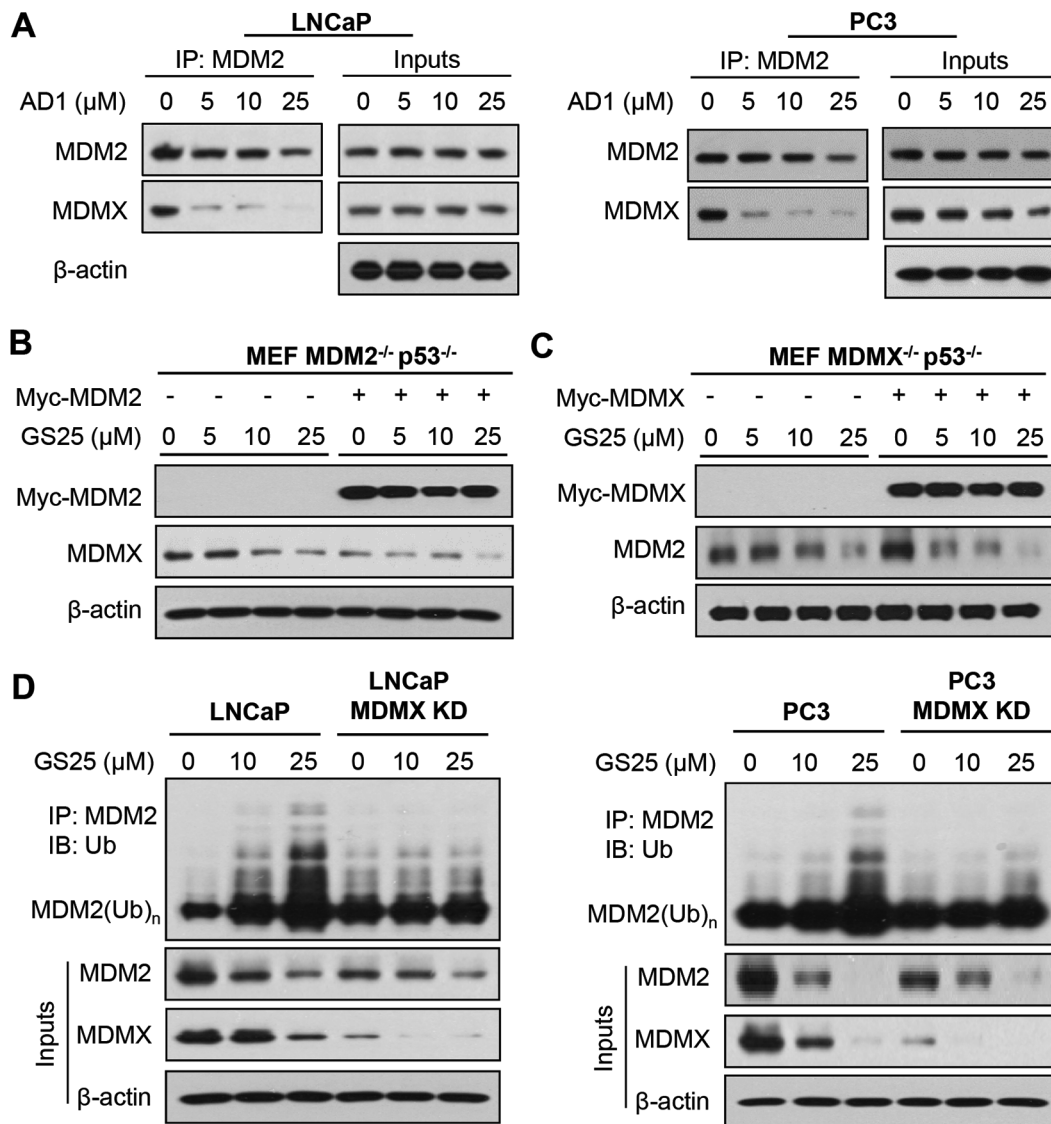
Figure 3. GS25 enhances MDM2 auto-degradation by disrupting the MDM2–MDMX interaction. (**A**) LNCaP and PC3 cells were treated with GS25 at the indicated concentrations for 2 h, followed by the co-immunoprecipitation of the MDM2–MDMX complex with an anti-MDM2 antibody. The protein levels of MDM2 and MDMX were determined by Western blotting. (**B, C**) MEF MDM2$^{-/-}$ p53$^{-/-}$ and MEF MDMX$^{-/-}$ p53$^{-/-}$ cells were transfected with (B) a Myc-MDM2 plasmid and (C) a Myc-MDMX plasmid for 24 h, respectively, followed by a 24-h treatment with GS25 at the indicated concentrations. The expression levels of MDM2 and MDMX were determined by a Western blot analysis. (**D**) LNCaP and PC3 cells were transfected with MDMX siRNA or control siRNA for 36 h, followed by exposure to GS25 at the indicated concentrations for 24 h. Cell lysates were subjected to immunoprecipitation with an anti-MDM2 antibody. The ubiquitinated MDM2 was detected using an anti-ubiquitin antibody. Data are representative of three or more experiments.

GS25 treatment does not lead to host toxicity

To determine if high doses and repeated treatment with GS25 caused host toxicity in mice, we evaluated the changes in body weight as a surrogate marker of toxicity, and observed that there were no significant differences in the average body weights of the mice between the treatment groups, suggesting that the treatment did not lead to host toxicity (Figure 6A). In addition, we also performed histological studies of various tissues from WT mice after 24 weeks of treatment (5 days/week). As shown in Figure 6B, there were no significant differences in the histological findings among the treatment and control groups in any of the tissues examined (liver, kidneys, spleen and brain), indicating that GS25 does not appear to cause toxicity in these organs at the effective doses, even when administered repeatedly. Consistent results were obtained for TRAMP mice treated with a high dose (data not shown). After being normalized to

the body weight, none of the major organs (liver and kidneys) showed any significant differences among the treatment and vehicle groups (Figure 6C). Blood samples from WT mice were collected after treatment with GS25 for 24 weeks. The samples were analyzed for standard clinical parameters and biomarkers of liver and kidney function, such as the levels of AST, ALT, TBIL, BUN and CR. These biochemical analyses showed that GS25 treatment did not have any influence on these parameters, indicating there was no major host toxicity in these mice.

Discussion

In recent years, plant-derived products have become more widely accepted in Western culture, and many are suggested to have therapeutic benefits for cancer. We are interested in ginsenosides, which are the major active components derived from *Panax ginseng* (31). We have evaluated one such analog in our
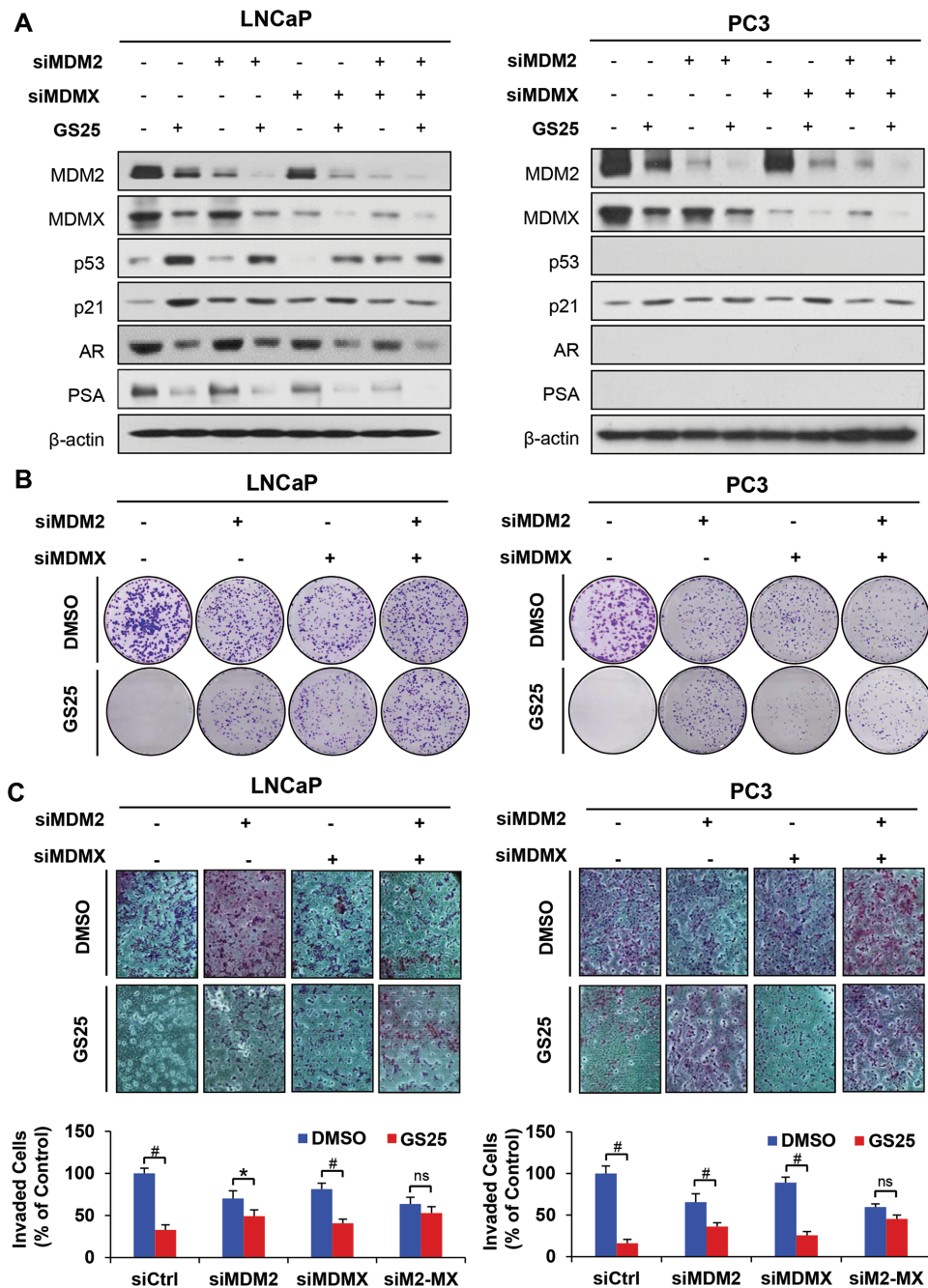
Figure 4. Knockdown of MDM2 or MDMX blocks GS25's anticancer activity. (**A–C**) LNCaP and PC3 cells were transfected with MDM2, MDMX or control siRNA for 36 h. The transfected cells were treated with GS25 at the indicated concentrations for 24 h for (A) assessment of the expression levels of various proteins by Western blotting, (B) the colony formation assay and (C) the transwell invasion assay. Data are representative of three or more experiments. (*P < 0.05, #P < 0.01 and 'ns' denotes 'not significant') siM2-MX: dual siRNAs against MDM2 and MDMX.

laboratory. From our initial studies, we found that GS25 has the strongest cytotoxic activity and antimetastatic effects among the known ginsenosides in several different cancer cell lines, including human prostate cancer cells. In addition, we found that the ginsenoside also affects oncoproteins, including MDM2.

The MDM2 oncogene is important in the progression of prostate cancer (10,11). It has also been found that MDM2 promotes angiogenesis by regulating the HIF1α, NFκB and STAT3 pathways in prostate cancer (24,25). The results from our laboratory's previous research (37) have demonstrated that knockdown of MDM2 results in tumor growth inhibition in prostate cancer *in*

vitro and *in vivo*, independent of the p53 and AR status, strongly supporting this concept. The existing MDM2 inhibitors, such as nutlin-3, RITA and MI219 (28), depend on the presence of wild-type p53 in cancer cells, and have little or no effect on cancer cells with mutant p53. This is because MDM2 also exerts a variety of p53-independent tumorigenic/pro-proliferative effects.

In this study, we demonstrated that GS25 is a first-in-the-class MDM2 inhibitor with unique mechanisms of action. GS25 directly bound the C-terminal RING domain of MDM2 and inhibited MDM2 by disrupting the MDM2–MDMX interaction and promoting MDM2 ubiquitination. Our results suggested that GS25
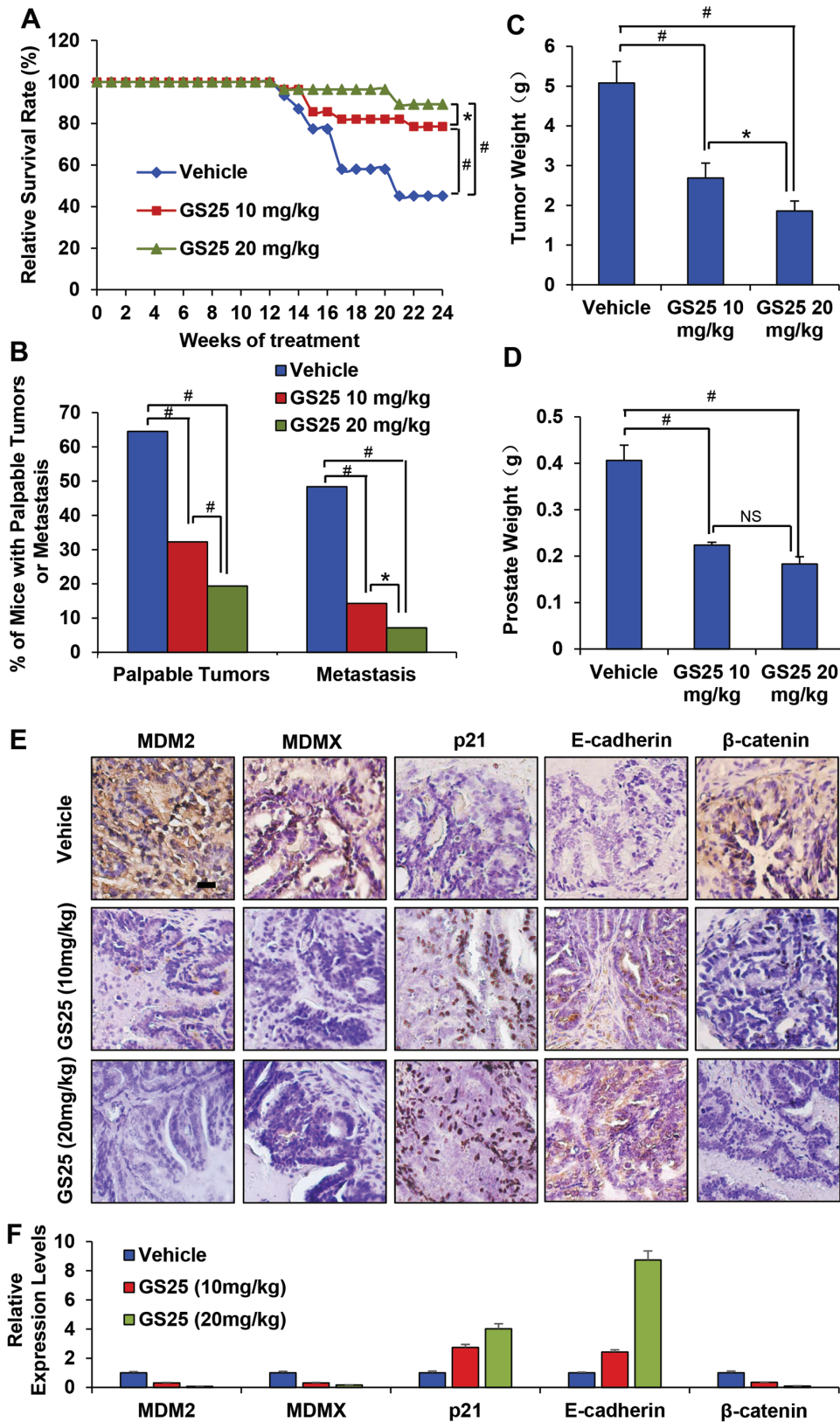
Figure 5. GS25 inhibits prostate tumorigenesis and metastasis in the TRAMP model. (**A**) Survival curves of the control and treatment groups in 28-week TRAMP mice. (**B**) The incidence of palpable tumors and metastatic lymph nodes in the 28-week-old mice in the vehicle control, 10 mg/kg GS25 and 20 mg/kg GS25 groups. (**C**) The weights of tumors at the time of euthanasia or upon termination of the experiment (28 weeks). (**D**) The prostate weights of mice from the vehicle control and GS25 treatment groups (mice with neuroendocrine carcinomas were excluded). (**E**) Representative immunohistochemistry staining for MDM2, MDMX, p21, E-cadherin and β-catenin in the prostates of 28-week-old vehicle control and GS25-treated TRAMP mice. (**F**) Quantification of positive staining density of markers in each group using ImageJ.
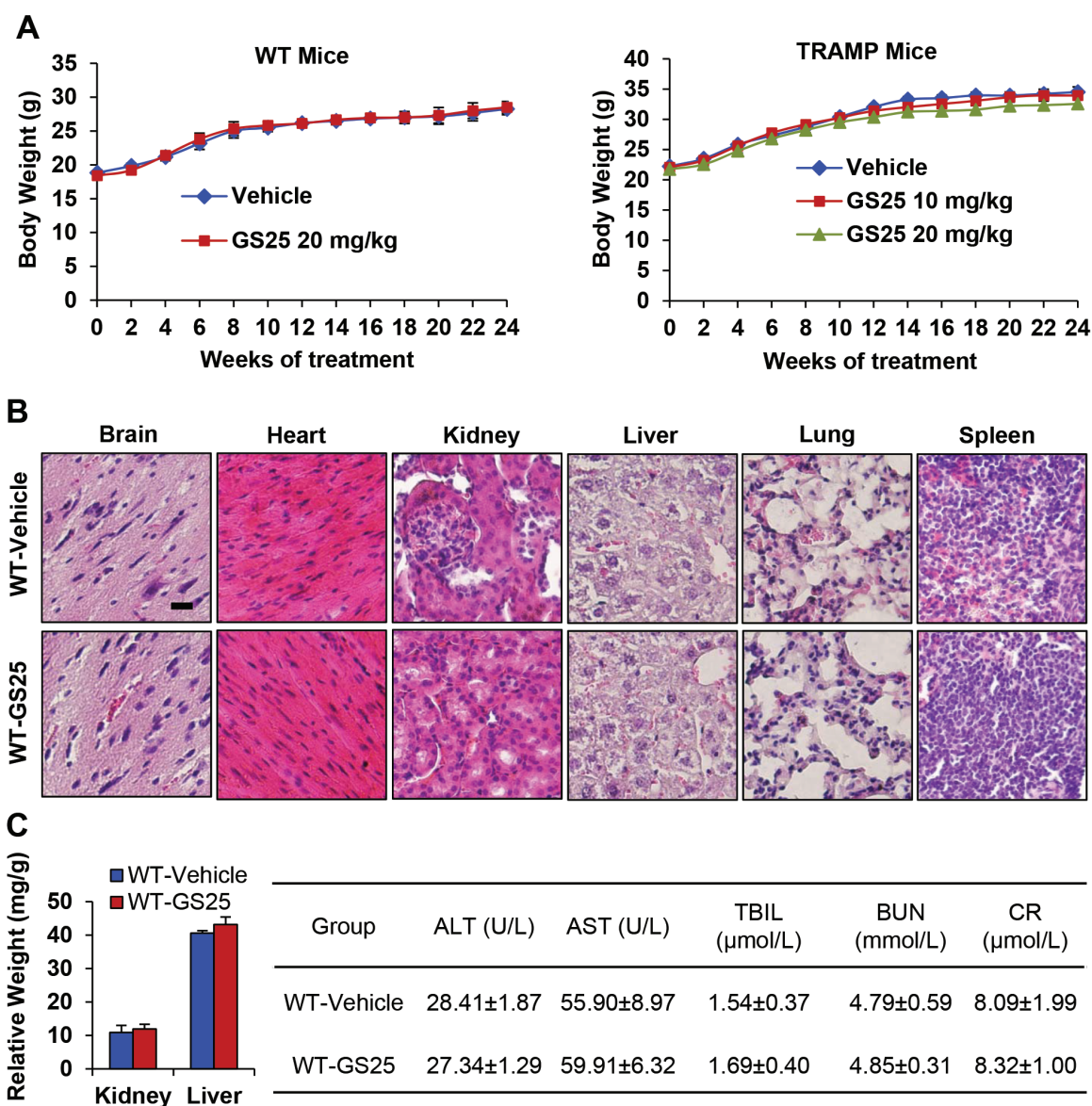
Figure 6. GS25 treatment does not lead to host toxicity. GS25 was administered by i.p. injection at 20 mg/kg to WT mice or at 10 or 20 mg/kg/day for 24 weeks to TRAMP mice. (**A**) The animals were monitored for changes in body weight as a surrogate marker for toxicity. (**B**) At the end of the experiment, HE staining was performed on various tissues from the WT mice. (**C**) The organ weights of WT mice (left panel; normalized to the body weight) and the effects of GS25 treatment on plasma indicators of toxicity (right panel). WT mice were treated with GS25 (20 mg/kg, 5 days/week) from 5 to 28 weeks of age. Plasma was separated from whole blood and stored at −80°C until it was analyzed. AST, aspartate amino transferase; ALT, alanine amino transferase; BUN, blood urea nitrogen; CR, creatinine; TBIL, total bilirubin.

directly targeted the MDM2 protein and exerted anticancer activities against cells with and without functional p53, indicating that it may be effective against a broader range of tumors with different genetic backgrounds. In addition, we found that the GS25-induced anticancer activity was dependent on MDM2 inhibition. Prostate cancer cells transfected with siRNA targeting MDM2 were much less responsive to GS25 treatment, suggesting that GS25 specifically targets MDM2.

Since the acquisition of androgen independence is an essential step in the progression of prostate cancer to advanced disease (which is resistant to further therapy), knowledge of this process has important clinical significance (38). In this study, our results showed that GS25 treatment or MDM2 knockdown inhibited the growth and metastasis of prostate cancer cells in an androgen-independent manner. There have also been reports that MDM2 is overexpressed during the development of androgen independence, and that MDM2 facilitates androgen receptor degradation

through its E3 ligase activity and reduces AR-mediated gene transcription (39). These studies provide a more thorough understanding of prostate cancer progression and the development of androgen independence, and also further establish MDM2 as a target for prostate cancer prevention and therapy.

Several ginseng compounds have been shown to have cancer preventive and therapeutic effects in epidemiological studies and several cancer models, but the studies investigating the use of other ginsenosides for prostate cancer have been limited. Moreover, most of the studies of ginsenosides have focused on the effects of the compounds on cancer cell lines, rather than *in vivo* models of cancer. The present study represented the first attempt to demonstrate the preventive effects of a ginsenoside against primary prostate cancers in transgenic mice. The transgenic adenocarcinoma of the mouse prostate (TRAMP) model is a widely used and highly efficient transgenic mouse model (40). Although this model has its drawbacks, notably the expression of a non-clinically relevant

transgene to induce the tumor formation and a lack of consensus about which region(s) of the mouse prostate best correspond to the human prostate (41), it does represent a tumor model which develops and progresses in a manner similar to the human disease (41). In this study, we demonstrated that GS25 could be safely and effectively used to prevent primary prostate cancers in TRAMP mice. Our preliminary data also indicated that GS25 did not appear to cause toxicity in any of the organs examined at the effective doses. Moreover, we found that MDM2 was overexpressed in the prostate cancer tissues of TRAMP mice. Thus, MDM2 overexpression may promote prostate cancer progression, and MDM2 inhibition or knockdown may lead to cancer prevention.

Although the cancer preventive activities of GS25 have been demonstrated in this study, additional studies are necessary to confirm its efficacy and safety in other models of prostate cancer, including orthotopic metastatic models and primary tumor-derived models with different genetic backgrounds, as well as other transgenic models of prostate cancer. In addition, in-depth pharmacokinetic and pharmacodynamic and pre-IND toxicity studies are needed to further develop the compound toward clinical translation.

In summary, we have herein demonstrated that GS25 can be utilized as a safe and effective agent for prostate cancer prevention and that its functions appear to be mediated by its inhibition of the MDM2 oncogene. These efficacy and mechanistic studies may provide proof-of-principle data to support the therapeutic value of this targeting strategy in future drug discovery.

Supplementary Material

Supplementary materials can be found at *Carcinogenesis* online.

Funding

Conflict of Interest Statement: None declared.

References

1. Siegel, R.L. *et al.* (2017) Cancer statistics, 2017. CA. Cancer J. Clin., 67, 7–30.
2. Trewartha, D. *et al.* (2013) Advances in prostate cancer treatment. Nat. Rev. Drug Discov., 12, 823–824.
3. Aly, A. *et al.* (2015) Understanding heterogeneity of treatment effect in prostate cancer. Curr. Opin. Oncol., 27, 209–216.
4. Lippman, S.M. *et al.* (2005) Designing the selenium and vitamin E Cancer Prevention Trial (SELECT). J. Natl. Cancer Inst., 97, 94–102.
5. Klein, E.A. *et al.* (2011) Vitamin E and the risk of prostate cancer: the Selenium and Vitamin E Cancer Prevention Trial (SELECT). JAMA, 306, 1549–1556.
6. Thompson, I.M. Jr *et al.* (2013) Long-term survival of participants in the prostate cancer prevention trial. N. Engl. J. Med., 369, 603–610.
7. Andriole, G.L. *et al.*; REDUCE Study Group. (2010) Effect of dutasteride on the risk of prostate cancer. N. Engl. J. Med., 362, 1192–1202.
8. Liss, M.A. *et al.* (2018) Prostate cancer prevention with 5-alpha reductase inhibitors: concepts and controversies. Curr. Opin. Urol., 28, 42–45.
9. Theoret, M.R. *et al.* (2011) The risks and benefits of 5α-reductase inhibitors for prostate-cancer prevention. N. Engl. J. Med., 365, 97–99.
10. Santarius, T. *et al.* (2010) A census of amplified and overexpressed human cancer genes. Nat. Rev. Cancer, 10, 59–64.
11. Leite, K.R. *et al.* (2001) Abnormal expression of MDM2 in prostate carcinoma. Mod. Pathol., 14, 428–436.
12. Levine, A.J. (1997) p53, the cellular gatekeeper for growth and division. Cell, 88, 323–331.
13. Oliner, J.D. *et al.* (1993) Oncoprotein MDM2 conceals the activation domain of tumour suppressor p53. Nature, 362, 857–860.
14. Wu, X. *et al.* (1993) The p53-mdm-2 autoregulatory feedback loop. Genes Dev., 7(7A), 1126–1132.
15. Haupt, Y. *et al.* (1997) Mdm2 promotes the rapid degradation of p53. Nature, 387, 296–299.
16. Kubbutat, M.H. *et al.* (1997) Regulation of p53 stability by Mdm2. Nature, 387, 299–303.
17. Zhang, Z. *et al.* (2005) p53-independent activities of MDM2 and their relevance to cancer therapy. Curr. Cancer Drug Targets, 5, 9–20.
18. Bouska, A. *et al.* (2008) Mdm2 promotes genetic instability and transformation independent of p53. Mol. Cell. Biol., 28, 4862–4874.
19. Bohlman, S. *et al.* (2014) p53-independent effects of Mdm2. Subcell. Biochem., 85, 235–246.
20. Bianco, R. *et al.* (2004) Combined targeting of epidermal growth factor receptor and MDM2 by gefitinib and antisense MDM2 cooperatively inhibit hormone-independent prostate cancer. Clin. Cancer Res., 10, 4858–4864.
21. Agus, D.B. *et al.* (1999) Prostate cancer cell cycle regulators: response to androgen withdrawal and development of androgen independence. J. Natl. Cancer Inst., 91, 1869–1876.
22. Pollack, A. *et al.* (2014) A tissue biomarker-based model that identifies patients with a high risk of distant metastasis and differential survival by length of androgen deprivation therapy in RTOG protocol 92-02. Clin. Cancer Res., 20, 6379–6388.
23. Khor, L.Y. *et al.* (2009) MDM2 and Ki-67 predict for distant metastasis and mortality in men treated with radiotherapy and androgen deprivation for prostate cancer: RTOG 92-02. J. Clin. Oncol., 27, 3177–3184.
24. Muthumani, P. *et al.* (2014) Pro-angiogenic effects of MDM2 through HIF-1α and NF-κB mediated mechanisms in LNCaP prostate cancer cells. Mol. Biol. Rep., 41, 5533–5541.
25. Rathinavelu, A. *et al.* (2012) A novel regulation of VEGF expression by HIF-1α and STAT3 in HDM2 transfected prostate cancer cells. J. Cell. Mol. Med., 16, 1750–1757.
26. Rayburn, E.R. *et al.* (2009) Recent advances in validating MDM2 as a cancer target. Anticancer. Agents Med. Chem., 9, 882–903.
27. Nag, S. *et al.* (2014) Targeting MDM2-p53 interaction for cancer therapy: are we there yet? Curr. Med. Chem., 21, 553–574.
28. Shangary, S. *et al.* (2008) Targeting the MDM2-p53 interaction for cancer therapy. Clin. Cancer Res., 14, 5318–5324.
29. Basmadjian, C. *et al.* (2014) Cancer wars: natural products strike back. Front. Chem., 2, 20.
30. Pascolutti, M. *et al.* (2014) Natural products as lead structures: chemical transformations to create lead-like libraries. Drug Discov. Today, 19, 215–221.
31. Nag, S.A. *et al.* (2012) Ginsenosides as anticancer agents: *in vitro* and *in vivo* activities, structure-activity relationships, and molecular mechanisms of action. Front. Pharmacol., 3, 25.
32. Zhao, Y. *et al.* (2007) Isolation, structural determination, and evaluation of the biological activity of 20(S)-25-methoxyl-dammarane-3beta, 12beta, 20-triol [20(S)-25-OCH3-PPD], a novel natural product from Panax notoginseng. Med. Chem., 3, 51–60.
33. Wang, W. *et al.* (2008) 20(S)-25-methoxyl-dammarane-3beta, 12beta, 20-triol, a novel natural product for prostate cancer therapy: activity *in vitro* and *in vivo* and mechanisms of action. Br. J. Cancer, 98, 792–802.
34. Uphoff, C.C. *et al.* (2005) Detection of mycoplasma contaminations. Methods Mol. Biol., 290, 13–23.
35. Wang, W. *et al.* (2014) The pyrido[b]indole MDM2 inhibitor SP-141 exerts potent therapeutic effects in breast cancer models. Nat. Commun., 5, 5086.
36. Voruganti, S. *et al.* (2015) RYBP predicts survival of patients with non-small cell lung cancer and regulates tumor cell growth and the response to chemotherapy. Cancer Lett., 369, 386–395.

37. Zhang, Z. *et al.* (2003) Antisense therapy targeting MDM2 onco-gene in prostate cancer: effects on proliferation, apoptosis, multiple gene expression, and chemotherapy. Proc. Natl Acad. Sci. USA, 100, 11636–11641.

38. Nandana, S. *et al.* (2014) Prostate cancer progression and metastasis: potential regulatory pathways for therapeutic targeting. Am. J. Clin. Exp. Urol., 2, 92–101.

39. Gaughan, L. *et al.* (2005) Regulation of androgen receptor and histone deacetylase 1 by Mdm2-mediated ubiquitylation. Nucleic Acids Res., 33, 13–26.

40. Greenberg, N.M. *et al.* (1995) Prostate cancer in a transgenic mouse. Proc. Natl Acad. Sci. USA, 92, 3439–3443.

41. Hurwitz, A.A. *et al.* (2001) The TRAMP mouse as a model for prostate cancer. Curr. Protoc. Immunol., Chapter 20, 20.5.1–20.5.23.